International Journal of Electrical and Electronic Engineering & Telecommunications

ISSN 2319 – 2518 www.ijeetc.com
Vol. 3, No. 2, April 2014

Research Paper

FIVE LEVEL INVERTER FOR OFF GRID CONNECTED PV SYSTEM EMPLOYING PI AND PID CONTROLLERS

R Narendra Rao[1]* and V Ganesh[1]

*Corresponding Author: R Narendra Rao, ✉ narendra.rnr@gmail.com

This paper presents a single-phase five-level inverter topology for grid-connected PV systems with a novel Pulse Width-Modulated (PWM) control scheme. Two reference signals identical to each other with an offset equivalent to the amplitude of the triangular carrier signal were used to generate PWM signals for the switches. A proportional-integral current control algorithm is implemented in MATLAB/SIMULINK to keep the current injected into the grid sinusoidal and to have high dynamic performance with rapidly changing atmospheric conditions. The inverter offers much less total harmonic distortion and can operate at near-unity power factor. A Proportional Integral (PI) current control algorithm is implemented to optimize the performance of the inverter. Simulation results indicate that the Total Harmonic Distortion (THD) of the five level inverter is much lesser than that of the conventional three-level inverter. Further, both the grid voltages and grid current are in phase at near-unity power factor.

Keywords: PWM inverter, Grid connected, Photovoltaic system, Proportional integral, Current control, PID control

INTRODUCTION

The demand for renewable energy has increased over the years because of shortage of fossil fuels and greenhouse effect. Among various types of renewable energy sources. Solar energy and wind energy have become very popular and demanding due to advancement in power electronics techniques. Photovoltaic (PV) sources are used today in many applications as they have the advantages of being maintenance and pollution free. Solar electric energy demand has grown consistently by 20%-25% per annum over the past 20 years, which is mainly due to the decreasing costs and prices. This decline has been driven by the following factors:

[1] Department of EEE, JNTUACE, Pulivendula, AP, India.

- An increasing efficiency of solar cells
- Manufacturing-technology improvements
- Economies of scale

PV inverter, which is the heart of a PV system, is used to convert dc power obtained from PV modules in to ac power to be fed in to the grid. Improving the output waveform of the inverter reduces its respective harmonic content and hence the size of the filter used and the level of Electromagnetic Interference (EMI) generated by switching operation of the inverter. In recent years, multilevel inverters have become more attractive for researchers and manufactures due to their advantages over conventional three-level Pulse Width-Modulated (PWM) inverters. They offer improved output waveforms, smaller filter size, lower EMI, lower Total Harmonic Distortion (THD).

The inverter is used in a PV system, a Proportional Integral (PI) current control scheme is employed to keep the output current sinusoidal and to have high dynamic performance under rapidly changing atmospheric conditions and to maintain the power factor at near unity. Similarly PV system for Proportional Integral Derivative (PID) current control scheme is employed to keep the output current sinusoidal and to have high dynamic performance and improve steady state stability. Many control strategies are proposed for five level inverter for off grid connected PV system renewable energy has increased significantly over the years because of shortage of fossil fuels and greenhouse effect. Among various types of renewable energy sources, solar energy and wind energy have become very popular and demanding due to advancement in power electronics techniques. Photovoltaic (PV) sources are used today in many applications as they have the advantages of being maintenance and pollution free. About economies of scale are discussed in Carrasco *et al.* (2006). The size of the filter used and the level of Electromagnetic Interference (EMI) generated by switching operation of the inverter are discussed in Agelidis *et al.* (1997).

In recent years, multilevel inverters have become more attractive for researchers and manufacturers due to their advantages over conventional three-level Pulse Width-Modulated (PWM) inverters. About the Pulse Width Modulation (PWM), Electromagnetic Interference (EMI), a general circuit topology of multilevel inverter and total harmonic distortion were proposed in the references (Choi *et al.*, 1991; Carrara *et al.*, 1992; Tolbert and Habetler, 1999; Calais *et al.*, 2001; Park *et al.*, 2003; and Kouro *et al.*, 2007). There are three common topologies for multilevel inverters about that cascaded H-bridge inverter, a non conventional power for plasma stabilization and operation of cascaded multilevel inverter are studied in the references (Marchesoni *et al.*, 1988; Rodriguez *et al.*, 2005; and Kou *et al.*, 2006). In addition, several modulation and control strategies have been developed or adopted for multilevel inverters, including the following: multilevel sinusoidal Pulse Width Modulation (PWM), multilevel selective harmonic elimination, and space vector modulation are studied in Rodriguez *et al.* (2002) and Kouro *et al.* (2007).

A control method to charge series-connected ultra electric double-layer capacitors suitable for photovoltaic generation

systems combining MPPT control method is referred in Mutoh and Inoue (2007). Comparison of photovoltaic array maximum power point tracking techniques is studied in Esram and Chapman (2007). Optimizing duty cycle perturbation of Maximum Power Point Tracking (MPPT) technique in the references (Femia *et al.*, 2004). An improved perturbation and observation maximum power point tracking algorithm for PV arrays in the reference (Liu and Lopes, 2004).

HARMONICS IN POWER SYSTEM AND CONTROLLERS

Voltage and current source harmonics imply power losses, Electromagnetic Interference (EMI) and pulsating torque in AC motor drives. Any periodic waveform can be shown to be the superposition of a fundamental and a set of harmonic components. By applying Fourier transformation, these components can be extracted. The frequency of each harmonic component is an integral multiple of its fundamental. There are several methods to indicate of the quantity of harmonics contents. The most widely used measure in North America is the Total Harmonics Distortion (THD), which is defined in terms of the amplitudes of the harmonics, H_n, at frequency nw_0, 2 where w_0 is frequency of the fundamental component whose amplitude of H1 and n is integer. The THD is mathematically given by

$$THD = \frac{\sqrt{\sum_{n=2}^{\infty} H_{(n)}^2}}{H_1}$$

PI AND PID CONTROLLERS

These two are conventional controllers that one has to know a mathematical model of the process in order to design a controller. Unconventional controllers utilize a new approaches to the controller design in which knowledge of a mathematical model of a process generally is not required. Manny industrial processes are nonlinear and thus complicate to describe mathematically. However, it is known that a good many nonlinear processes can satisfactory controlled using PID controllers providing that controller parameters are tuned well. Practical experience shows that this type of control has a lot of sense since it is simple and based on 3 basic behavior types: Proportional (P), Integrative (I) and Derivative (D). Instead of using a small number of complex controllers, a larger number of simple PID controllers is used to control simpler processes in an industrial assembly in order to automates the certain more complex process. PID controller and its different types such as P, PI and PD controllers are today basic building blocks in control of various processes.

PI Controller

PI controller will eliminate forced oscillations and steady state error resulting in operation of on-off controller and P controller respectively. However, introducing integral mode has a negative effect on speed of the response and overall stability of the system. Thus, PI controller will not increase the speed of response. It can be expected since PI controller does not have means to predict what will happen with the error in near future. This problem can be solved by introducing derivative mode which has ability to predict what will happen with the error in near future and thus to decrease a reaction time of the controller.

PI controllers are very often used in industry, especially when speed of the response is not an issue. A control without D mode is used when:

- Fast response of the system is not required.
- Large disturbances and noise are present during operation of the process.
- There is only one energy storage in process (capacitive or inductive).
- There are large transport delays in the system.

PID Controller

PID controller has all the necessary dynamics: fast reaction on change of the controller input (D mode), increase in control signal to lead error towards zero (I mode) and suitable action inside control error area to eliminate oscillations (P mode). Derivative mode improves stability of the system and enables increase in gain *K* and decrease in integral time constant *Ti*, which increases speed of the controller response. PID controller is used when dealing with higher order capacitive processes (processes with more than one energy storage) when their dynamic is not similar to the dynamics of an integrator (like in many thermal processes). PID controller is often used in industry, but also in the control of mobile objects (course and trajectory following included) when stability and precise reference following are required. Conventional autopilot is for the most part PID type controllers.

- Use K_P to decrease the rise time.
- Use K_D to reduce the overshoot and settling time.
- Use K_I to eliminate the steady-state error.

FIVE-LEVEL INVERTER TOPOLOGY AND PWM

The proposed single-phase five-level inverter topology is shown in Figure 1. The inverter adopts a full-bridge configuration with an auxiliary circuit. PV arrays are connected to the inverter via a dc-dc boost converter. Because the proposed inverter is used in a grid-connected PV system, utility grid is used instead of load. The dc-dc boost converter is used to step up inverter output voltage V_{inv} to be more than $\sqrt{2}$ of grid voltage V_g to ensure power flow from the PV arrays into the grid. A filtering inductance *Lf* is used to filter the current injected into the grid. The injected current must be sinusoidal with low harmonic distortion. In order to generate sinusoidal current, sinusoidal PWM is used because it is one of the most effective methods. Sinusoidal PWM is obtained by comparing a high-frequency carrier with a low-frequency sinusoid, which is the modulating or reference signal.

Figure 1: Single Phase Five Level Inverter

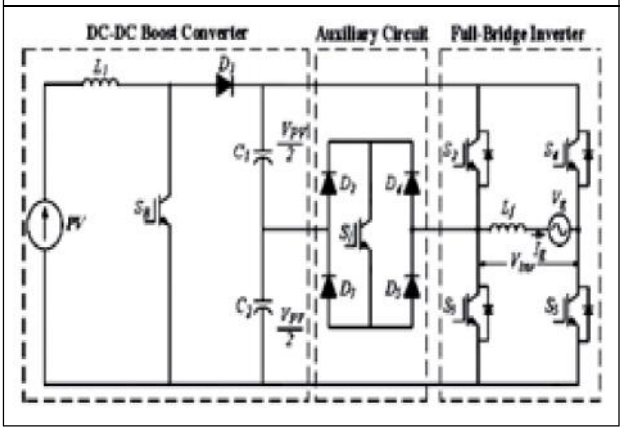

SINUSOIDAL PWM LAW

A fundamental period consists of *p* pulses whose widths vary sinusoidally throughout the cycle to give the fundamental component of frequency. The basis of equivalence between

the desired sinusoid and the actual pulsed waveform is taken to be volt-seconds, as shown in Figure 1, i.e., $A_{S1} = A_{p1}$ *and* $A_{S2} = A_{p2}$. One of these pulses, the general k^{th} pulse, is characterized in detail in Figure 5.

The switching period Δ and the frequency modulation ratio p are, respectively, given by

$$\Delta = \frac{2®}{p} \quad ...(1)$$

$$p = \frac{f_s}{f_1} \quad ...(2)$$

where f_s is the switching frequency and f_1 is the fundamental frequency. The quarter period of pulse $¢_0$ is given as

$$¢_0 = \frac{\Delta}{4} \quad ...(3)$$

$~_K$ is the position from the origin of the fundamental period of the midpoint of the period Δ. The angles $¢_{1K}$ and $¢_{2K}$ are the modulating angles which vary throughout the cycle and it is to calculate these angles that a modulation law must be derived. Consider first the average voltages V_{1K} and V_{2K} during the two halves of the modulating pulse

$$V_{1k} = \frac{(V_s)\{¢_{1k} - (2¢_0 - ¢1k)\}}{2¢_0} \quad ...(4)$$

$$V_{1K} = \frac{(V_S)(¢_{1K} - ¢_0)}{¢_0} \quad ...(5)$$

$$= (V_s)_{\ 1k} \quad ...(6)$$

where

$$_{1k} = \frac{(¢_{1k} - ¢_0)}{¢_0} \quad ...(7)$$

and, similarly

$$V_{2k} = (V_s)_{\ 2k} \quad ...(8)$$

where

$$_{2k} = \frac{(¢_{2k} - ¢_0)}{¢_0} \quad ...(9)$$

The volt-second A_{S1} is the half-pulse width of the sine wave and is given according to Figure 1 by

$$A_{S1} = \int_{~k-2¢0}^{~k} Vm \sin^{-} d^{-} \quad ...(10)$$

$$= 2V_M \sin¢_0 \sin(~_k - ¢_0) \quad ...(11)$$

However, $\sin¢_0 \to ¢_0$ when $¢_0$ is small

$$A_{s1} = 2¢_0 V_m \sin(~_k - ¢_0) \quad ...(12)$$

and, similarly,

$$A_{s2} = 2¢_0 V_m \sin(~_k + ¢_0) \quad ...(13)$$

For the corresponding volt-second A_{P1}, in the PWM waveform,

$$A_{p1} = 2¢_0 V_{1K} \quad ...(14)$$

$$A_{P1} = 2¢_{0\ \ 1K}(V_S) \quad ...(15)$$

and, similarly,

$$A_{P2} = 2¢_{0\ \ 2K}(V_S) \quad ...(16)$$

For equivalence of volt-seconds from which the modulation law can be derived, we require that

$$A_{S1} = A_{P1} \quad ...(17)$$

$$A_{S2} = A_{P2} \quad ...(18)$$

By Equating (12) and (14), and (13) and (16)

$$_{1K} = M \sin(~_K - ¢_0) \quad ...(19)$$

and, similarly,

$$_{2K} = M \sin(~_k + ¢_0) \quad ...(20)$$

where M is the “modulation index” and

$$M = \frac{V_m}{V_s} \quad ...(21)$$

Equation (21) can be expressed in terms of amplitude of carrier signal V_c by replacing V_s with V_c. Because, in this topology, two identical reference signals are used,

$V_S = 2V_C$ and

$V_m = V_{ref1} = V_{ref2}$

The switching angles,

$$¢_{1k} = ¢_0[1 + M(~_k - ¢_0)]$$

$$¢_{2k} = ¢_0[1 + M\sin(~_k + ¢_0)] \quad ...(22)$$

The harmonics due to the k^{th} pulse alone, A_{nk}, and then summating the harmonic contributions of all p pulses

$$A_{nk}k = 1/2® = \int_{~K-2¢0}^{~K_+2¢0} V(¯)e - jn¯ d¯$$

where $V(¯)$ is the voltage pulse shown in Figure 5

$$A_{nk} = \frac{1}{2®}\{- \int_{~k-2¢0}^{~k-¢1k} Vse - jn¯ d¯$$

$$\int_{~k-¢1k}^{~k+¢2k} Vse - jn¯ d¯ - \int_{~k+2¢k}^{~k+2¢0} Vse - jn¯ d¯\} \quad ...(23)$$

$$= (V_S)(\frac{1}{2®})(\frac{-2}{jn})$$

$$\times \begin{Bmatrix} e - jn¢_{2k} \\ - ejn¢_{1k} + j\sin 2n¢_0 \end{Bmatrix} e - jn~_k \quad ...(24)$$

Equation (25) cannot be readily simplified. Therefore, for the harmonic amplitudes due to all p pulses in a fundamental cycle

$$A_n = \sum_{k=1}^{p} A_{nk} \quad ...(25)$$

Mathematical Formulation

The PI algorithm can be expressed in the continuous time domain as

$$u(t) = K_{pe(t)} + Ki \int_{²=0}^{t} e(²)d² \quad ...(26)$$

where

$u(t)$ control signal;

$e(t)$ error signal;

t continuous-time-domain time variable;

$²$ calculus variable of integration;

K_p proportional-mode control gain;

integral-mode control gain.

Implementing this algorithm using a PWM requires one to transform it into the discrete-time domain. Trapezoidal sum approximation is used to transform the integral term into the discrete-time domain because it is the most straight forward technique. The proportional term is directly used without approximation.

P term: $K_{pe(t)} = K_{pe(k)}$ ...(27)

Iterm: $Ki \int_{²=0}^{t} e(²)d² \cong Ki$

$$\sum_{i=0}^{k} h/2[e(i) + e(i-1)] \quad ...(28)$$

Time relationship: $t = k \times h$

where

h sampling period;

k discrete-time index: $k = 0, 1, 2, ...$

For simplification, it is convenient to define new controller gains as

$$K = \frac{K_{IH}}{2} \quad ...(29)$$

From which one can construct the discrete-time PI control law as

$$u(k) = K_{pe}(t) + K_j \sum_{i=0}^{k} [e(i) + e(i-1)] \quad ...(30)$$

To eliminate the need to calculate the full summation at each time step (which would require an ever-increasing amount of computation as time goes on), the summation is expressed as a running sum

$$sum(k) = sum(k-1) + [e(k) + e(k-1)] \quad ...(31)$$

$$u(k) = K_{pe(k)} + K_j sum(k) \quad ...(32)$$

These two equations, which represent the discrete-time PI control law, are implemented in PWM to control the overall operation of the inverter.

OPERATIONAL PRINCIPLE OF THE PROPOSED INVERTER

Because PV arrays are used as input voltage sources, the voltage produced by the arrays is known as V_{arrays}. V_{arrays} is boosted by a dc-dc boost converter to exceed $\sqrt{2}$Vg. The voltage across the dc-bus capacitors is known as V_{pv}. The operational principle of the proposed inverter is to generate five level output voltage, i.e., 0, $+\frac{V_{pv}}{2}$, + V_{pv} $-\frac{V_{pv}}{2}$, and $-V_{pv}$ as in Figure 9. As shown in Figure 3, an auxiliary circuit which consists of four diodes and a switch S1 is used between the dc-bus capacitors and the full-bridge inverter. Proper switching control of the auxiliary circuit can generate half level of PV supply voltage, i.e., $+\frac{V_{PV}}{2}$ and $-\frac{V_{PV}}{2}$.

Table 1: Switching Table

S1	S2	S3	S4	S5	V_{inv}
ON	OFF	OFF	OFF	ON	+Vpv/2
OFF	ON	OFF	OFF	ON	+Vpv
OFF	OFF or (ON)	OFF or (ON)	ON or (OFF)	ON or (OFF)	0
ON	OFF	OFF	ON	OFF	–Vpv/2
OFF	OFF	ON	ON	OFF	–Vpv

Two reference signals V_{ref1} and V_{ref2} will take turns to be compared with the carrier signal at a time. If V_{ref1} exceeds the peak amplitude of the carrier signal Vcarrier, V_{ref2} will be compared with the carrier signal until it reaches zero. At this point onward, V_{ref1} takes over the comparison process until it exceeds Vcarrier. This will lead to a switching pattern, as shown in Figure 8. Switches S1-S3 will be switching at the rate of the carrier signal frequency, whereas S4 and S5 will operate at a frequency equivalent to the fundamental frequency. Table 1. I illustrates the level of Vinv during S1-S5 switch on and off.

RESULTS AND DISCUSSION

The work is carried out with the design of different controllers such as PI and PID controllers. The results are validated for these controllers.

With PI Controller

The inverter output voltage (V_{inv}) and grid current (i_g) for different modulation index with PI controller are shown in Figures 2 to 6.

In the above figures the modulation index M for PI controller will determine the shape of the inverter output voltage V_{inv} and the grid current I_g. A figure shows V_{inv} and I_g for different values of M. The dc-bus voltage is set at 200 V (>1.4 Vg) in this case (Vg is 120 V) in order

Figure 2: Grid Current (I_g) for M < 0.5

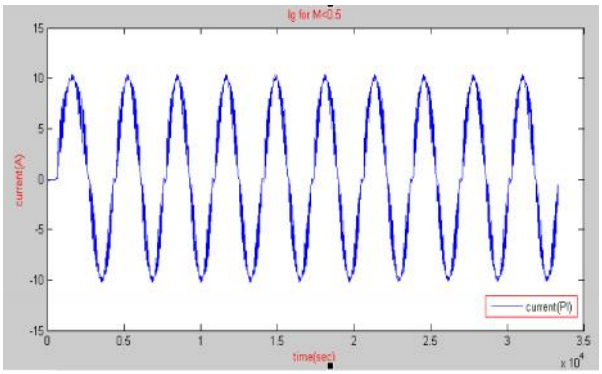

Figure 3: Inverter Output Voltage (V_{inv}) for M < 0.5

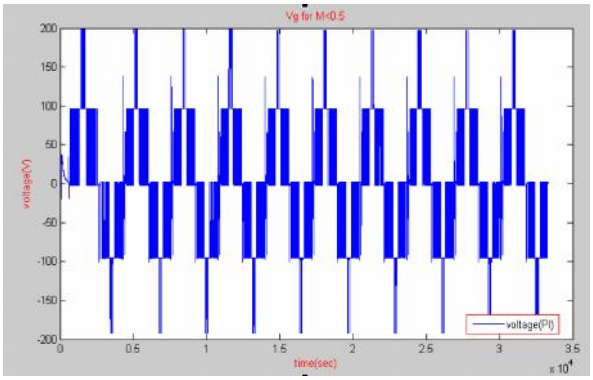

Figure 4: Grid Current (I_g) for M > 1

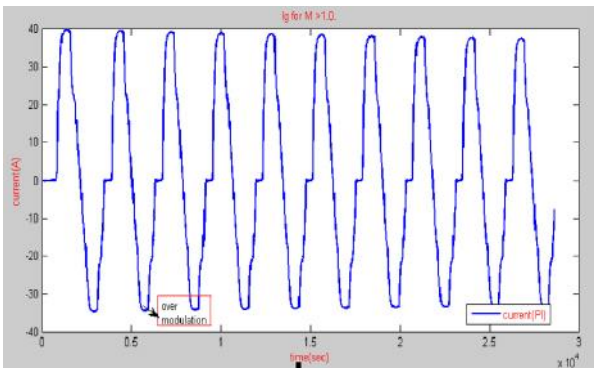

to inject current into the grid. Figure 2 shows that V_{inv} is less than 1.4 Vg due to M being less than 0.5. The inverter should not operate at this condition because the current will be injected from the grid into the inverter, rather

Figure 5: Inverter Output Voltage (V_{inv}) for M > 1

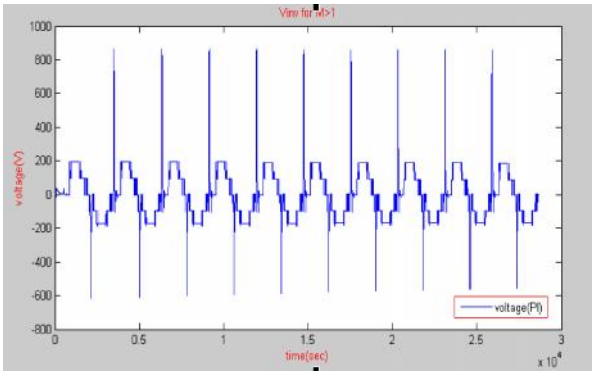

Figure 6: Inverter Output Voltage (V_{inv}) for 0.5 < M < 1

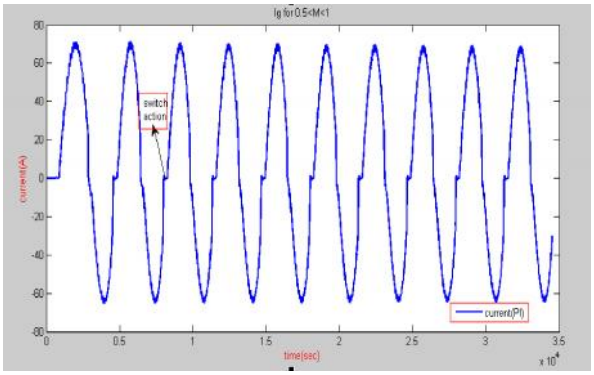

than the PV system injecting the current into the grid, as shown in Figure 2. Over modulation condition, which happens when M >1, is shown in Figure 4. It has a flat top at the peak of the positive and negative cycles because both the reference signals exceed the maximum amplitude of the carrier signal.

This will cause I_g to have a flat portion at the peak of the sine waveform, as shown in Figure 4. To optimize the power transferred from PV arrays to the grid, it is recommended to operate at $0.5 \leq M \leq 1.0$. V_{inv} and I_g for optimal operating condition are shown in Figures 6 and 7, respectively. As I_g is almost a pure sine wave, the THD can be reduced when compared with

that under other values of M in analytical controller as shown in Figure 6. To analyze the performance of the PI current control scheme, a sudden step change is applied to the simulation process. This step change is similar to real-time environment condition.

With PID Controller

The inverter output voltage (V_{inv}) and grid current (I_g) for different modulation index with PID controller are shown in Figures 8 to 13.

In the above figures the modulation index (M) for PID controller will determine the shape of the inverter output voltage V_{inv} and the grid current I_g. A figure shows V_{inv} and I_g for different values of M. The dc-bus voltage is set at 200 V (>1.4 Vg) in this case, (V_g is 120 V) in order to inject current into the grid. Figure 8 shows that V_{inv} is less than 1.4 Vg due to M being less than 0.5.

Figure 7: Grid Current (I_g) for M < 0.5 < 1

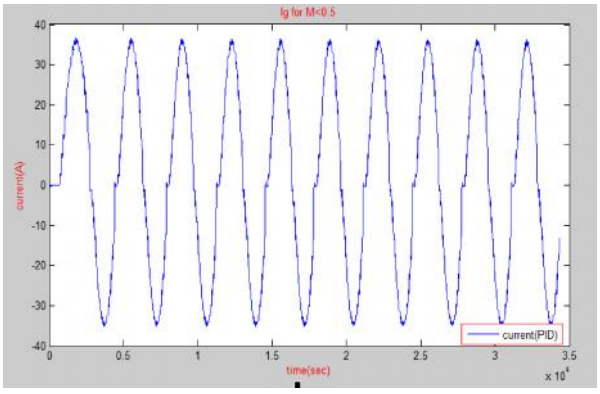

Figure 8: Grid Current (I_g) for M < 0.5

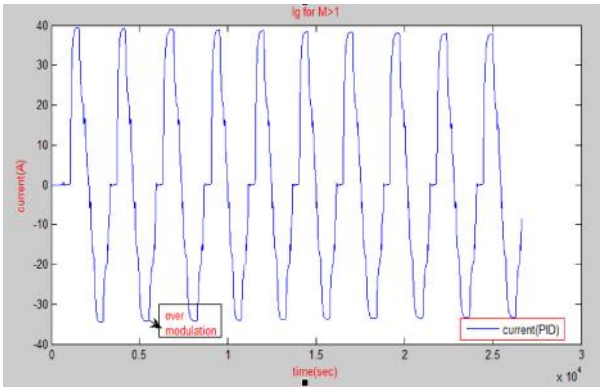

Figure 9: Inverter Output Voltage (V_{inv}) for M < 0.5

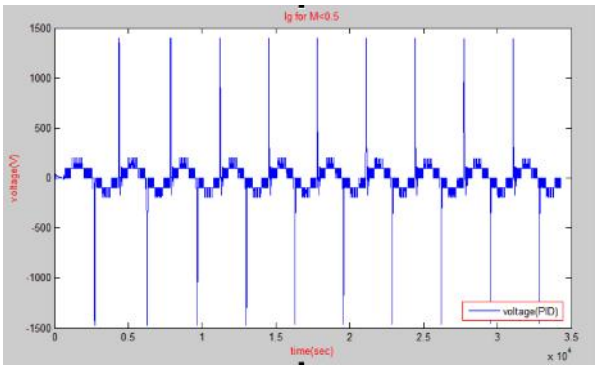

Figure 10: Grid Current (I_g) for M > 1

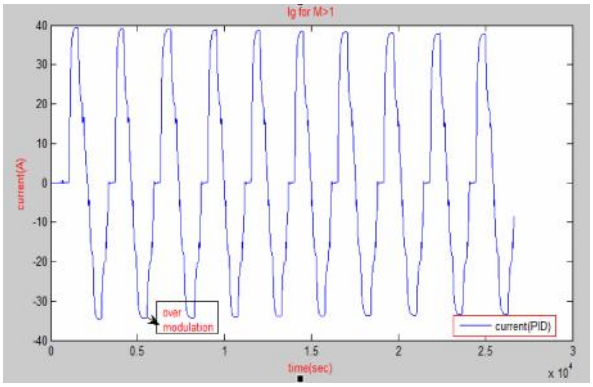

Figure 11: Inverter Output Voltage (V_{inv}) for M > 1

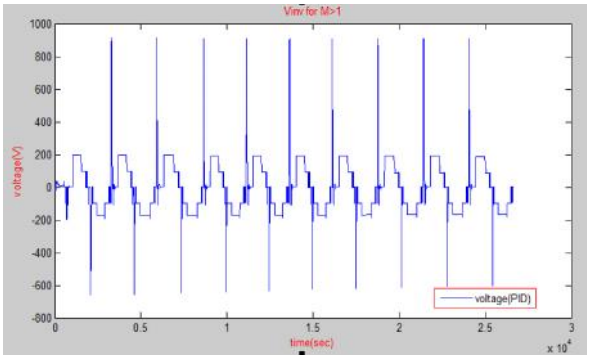

Figure 12: Grid Current (I_g) for M < 0.5 < 1

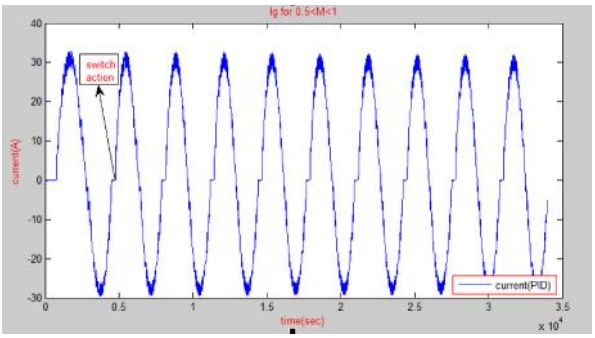

Figure 13: Inverter Output Voltage (V_{inv}) for M < 0.5 < 1

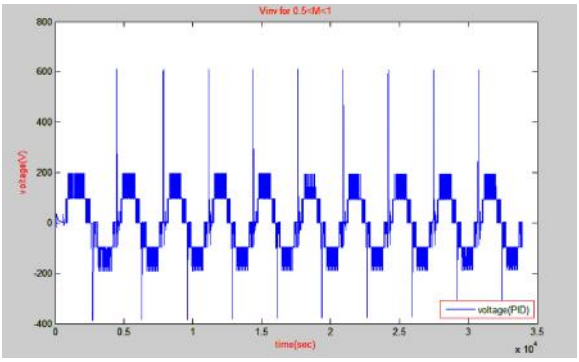

The inverter should not operate at this condition because the current will be injected from the grid into the inverter, rather than the PV system injecting the current into the grid, as shown in Figure 8. Over modulation condition, which happens when M >1, is shown in Figure 9. It has a flat top at the peak of the positive and negative cycles because both the reference signals exceed the maximum amplitude of the carrier signal. This will cause Ig to have a flat portion at the peak of the sine waveform, as shown in Figure 10. To optimize the power transferred from PV arrays to the grid, it is recommended to operate at $0.5 \leq M \leq 1.0$. V_{inv} and I_g for optimal operating condition are shown in Figures 12 and 13 respectively. As I_g is almost a pure sine wave, the THD can be reduced considerably when compared with that under other values of M analytical controller and PI controller.

After validating different controllers, i.e., analytical, PI and PID controllers, the results shows that Total harmonic distortion has been reduced considerably for PID controllers and the grid current (I_g) is almost a pure sine wave.

CONCLUSION

This paper deals with single phase five-level inverter with off grid connected and photovoltaic system. The results obtained by using five level inverter for off grid connected PV system with PI controller has improved output waveforms, smaller filter size, lower electromagnetic interference and low harmonic distortion when compared three level inverter for off grid connected PV system with PI controller. The thesis presented a single-phase five level inverter for PV application. It utilizes two reference signals and a carrier signal to generate PWM switching signals. However, no systematic analysis has been performed in order to determine basic properties of multi-phase PWM in general, and to establish close correlation between carrier based PWM and space vector PWM. THD of the five-level inverter is much lesser than that of the conventional three-level inverter. Furthermore, both the grid voltage and the grid current are in phase at near-unity power factor.

REFERENCES

1. Agelidis V G, Baker D M, Lawrance W B and Nayar C V (1997), “A Multilevel PWM Inverter Topology for Photovoltaic Applications”, in Proc. IEEE ISIE, pp. 589-594, Guimarães, Portugal.
2. Calais M, Borle L J and Agelidis V G (2001), “Analysis of Multicarrier PWM

Methods for a Single-Phase Five-Level Inverter", in Proc. 32nd Annu. IEEE PESC, Vol. 3, June 17-21, pp. 1173-1178.

3. Carrara G, Gardella S, Marchesoni M, Salutari R and Sciutto G (1992), "A New Multilevel PWM Method: A Theoretical Analysis", *IEEE Trans. Power Electron.*, Vol. 7, No. 3, pp. 497-505.
4. Carrasco J M, Franquelo L G, Bialasiewicz J T, Galvan E, PortilloGuisado R C, Prats M AM, Leon J I and Moreno-Alfonso N (2006), "Power-Electronic Systems for the Grid Integration of Renewable Energy Sources: A Survey", *IEEE Trans. Ind. Electron.*, Vol. 53, No. 4, pp. 1002-1016.
5. Choi N S, Cho J G and Cho G H (1991), "A General Circuit Topology of Multilevel Inverter", in Proc. 22nd Annu. IEEE PESC, June 24-27, pp. 96-103.
6. Esram T and Chapman P L (2007), "Comparison of Photovoltaic Array Maximum Power Point Tracking Techniques", *IEEE Trans. Energy Convers.*, Vol. 22, No. 2, pp. 439-449.
7. Femia N, Petrone G, Spagnuolo G and Vitelli M (2004), "Optimizing Duty Cycle Perturbation of P&O MPPT Technique", in Proc. 35th Annu. IEEE PESC, Vol. 3, June 20-25, pp. 1939-1944.
8. Kou X, Corzine K and Wielebski M (2006), "Over Distention Operation of Cascaded Multilevel Inverters", *IEEE Trans. Ind. Appl.*, Vol. 42, No. 3, pp. 817-824.
9. Kouro S, Rebolledo J and Rodriguez J (2007), "Reduced Switching-Frequency Modulation Algorithm for High-Power Multilevel Inverters", *IEEE Trans. Ind. Electron.*, Vol. 54, No. 5, pp. 2894-2901.
10. Liu X and Lopes L A C (2004), "An Improved Perturbation and Observation Maximum Power Point Tracking Algorithm for PV Arrays", in Proc. IEEE 35th Annu. PES.
11. Marchesoni M, Mazzucchelli M and Tenconi S (1988), "A non Conventional Power Converter for Plasma Stabilization", in Proc. IEEE Power Electron. Spec. Conf., pp. 122-129.
12. Mutoh N and Inoue T (2007), "A Control Method to Charge Series-Connected Ultra Electric Double Layer Capacitors Suitable for Photovoltaic Generation Systems Combining MPPT Control Method", *IEEE Trans. Ind. Electron.*, llVol. 54, No. 1, pp. 374-383.
13. Park S J, Kang F S, Lee M H and Kim C U (2003), "A New Single-Phase Five Level PWM Inverter Employing a Deadbeat Control Scheme", *IEEE Trans. Power Electron.*, Vol. 18, No. 18, pp. 831-843.
14. Rodriguez J, Hammond P, Pontt J, Musalem R, Lezana P and Escobar M (2005), "Operation of a Medium-Voltage Drive Under Faulty Conditions", *IEEE Trans. Ind.Electron.*, Vol. 52, No. 4, pp. 1080-1085.
15. Rodriguez J, Lai J-S and Peng F Z (2002), "Multicarrier PWM Strategies for Multilevel Inverters", *IEEE Trans. Ind. Electron.*, Vol. 49, No. 4, pp. 724-738.
16. Tolbert L M and Habetler T G (1999), "Novel Multilevel Inverter Carrier-Based PWM Method", *IEEE Trans. Ind. Appl.*, Vol. 35, No. 5, pp. 1098-1107.